Strong Superexchange in a $d^{9-\delta}$ Nickelate Revealed by Resonant Inelastic X-Ray Scattering

J. Q. Lin[1,2,3,4] P. Villar Arribi[5] G. Fabbris,[1,6] A. S. Botana,[7] D. Meyers,[1,8] H. Miao,[1,9] Y. Shen[1]
D. G. Mazzone[1,10] J. Feng[11,*] S. G. Chiuzbăian,[11,12] A. Nag,[13] A. C. Walters[13] M. García-Fernández,[13]
Ke-Jin Zhou,[13] J. Pelliciari[14] I. Jarrige,[14] J. W. Freeland[6] Junjie Zhang,[5,15] J. F. Mitchell[5] V. Bisogni,[14]
X. Liu,[2,†] M. R. Norman,[5,‡] and M. P. M. Dean[1,§]

[1]*Condensed Matter Physics and Materials Science Department, Brookhaven National Laboratory, Upton, New York 11973, USA*
[2]*School of Physical Science and Technology, ShanghaiTech University, Shanghai 201210, China*
[3]*Institute of Physics, Chinese Academy of Sciences, Beijing 100190, China*
[4]*University of Chinese Academy of Sciences, Beijing 100049, China*
[5]*Materials Science Division, Argonne National Laboratory, Lemont, Illinois 60439, USA*
[6]*Advanced Photon Source, Argonne National Laboratory, Lemont, Illinois 60439, USA*
[7]*Department of Physics, Arizona State University, Tempe, Arizona 85287, USA*
[8]*Department of Physics, Oklahoma State University, Stillwater, Oklahoma 74078, USA*
[9]*Material Science and Technology Division, Oak Ridge National Laboratory, Oak Ridge, Tennessee 37830, USA*
[10]*Laboratory for Neutron Scattering and Imaging, Paul Scherrer Institut, 5232 Villigen PSI, Switzerland*
[11]*Sorbonne Université, CNRS, Laboratoire de Chimie Physique-Matière et Rayonnement, UMR 7614,
4 place Jussieu, 75252 Paris Cedex 05, France*
[12]*Synchrotron SOLEIL, L'Orme des Merisiers, Saint-Aubin, BP 48, 91192 Gif-sur-Yvette, France*
[13]*Diamond Light Source, Harwell Science and Innovation Campus, Didcot, Oxfordshire OX11 0DE, United Kingdom*
[14]*National Synchrotron Light Source II, Brookhaven National Laboratory, Upton, New York 11973, USA*
[15]*Institute of Crystal Materials, Shandong University, Jinan, Shandong 250100, China*

The discovery of superconductivity in a $d^{9-\delta}$ nickelate has inspired disparate theoretical perspectives regarding the essential physics of this class of materials. A key issue is the magnitude of the magnetic superexchange, which relates to whether cuprate-like high-temperature nickelate superconductivity could be realized. We address this question using Ni L-edge and O K-edge spectroscopy of the reduced $d^{9-1/3}$ trilayer nickelates $R_4Ni_3O_8$ (where $R =$ La, Pr) and associated theoretical modeling. A magnon energy scale of ~80 meV resulting from a nearest-neighbor magnetic exchange of $J = 69(4)$ meV is observed, proving that $d^{9-\delta}$ nickelates can host a large superexchange. This value, along with that of the Ni-O hybridization estimated from our O K-edge data, implies that trilayer nickelates represent an intermediate case between the infinite-layer nickelates and the cuprates. Layered nickelates thus provide a route to testing the relevance of superexchange to nickelate superconductivity.

Ever since the discovery of superconductivity in the cuprates [1], researchers have been searching for related unconventional high-temperature (T_c) superconductors based on different transition metal ions [2–4]. Nickel, given its proximity to copper in the periodic table, represents an obvious target element. A popular concept has been to try to realize materials with $Ni^{1+}:3d^9$ ions with planar oxygen coordination residing in layers, as it was conjectured that this would mimic the strong magnetic superexchange that was proposed to be important for cuprate superconductivity [5]. The appropriateness of this assumption in layered $RNiO_2$ materials ($R =$ La, Pr, Nd) was, however, questioned, as the predicted increase in charge-transfer energy in $RNiO_2$, with respect to cuprates, would be expected to reduce the superexchange [6].

Superconductivity at a relatively modest $T_c \approx 15$ K in $Nd_{1-x}Sr_xNiO_2$ was nonetheless reported [7]. This has motivated many studies, often conflicting, concerning the nature of the normal-state electronic structure and correlations in these and related materials [8–30]. $RNiO_2$ materials are the infinite-layer members of a series of low-valence (with $d^{9-\delta}$ filling) layered nickelates $R_{n+1}Ni_nO_{2n+2}$, where n represents the number of NiO_2 layers per formula unit [31–34]. Given the important role of charge transfer and superexchange in many theories of unconventional superconductivity, determining trends for these quantities is highly important for understanding nickelate superconductivity and potentially discovering new nickelate superconductors [35,36]. Among the known members of this nickelate family, trilayer materials, shown
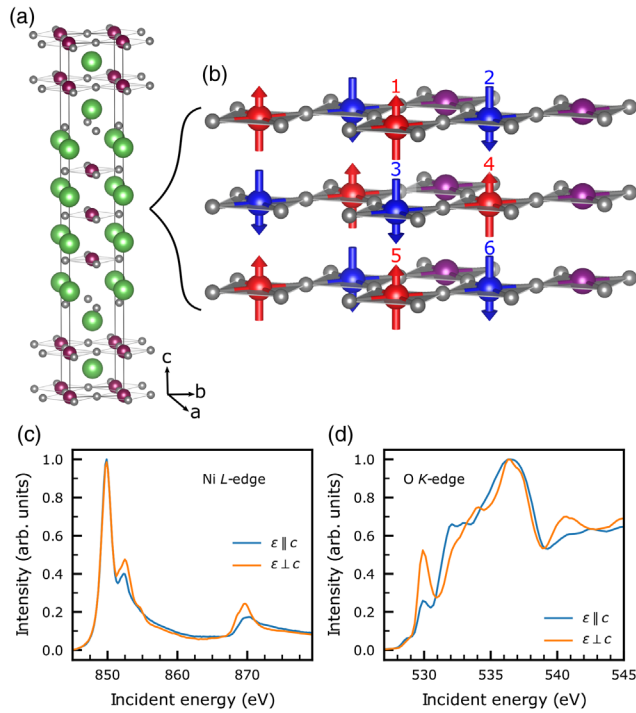
FIG. 1. Crystal structure and x-ray absorption spectrum (XAS). (a) Unit cell of $La_4Ni_3O_8$ and $Pr_4Ni_3O_8$ with Ni in purple, O in gray, and La/ Pr in green [39]. (b) The active trilayer nickel-oxide planes in $La_4Ni_3O_8$ with an illustration of the diagonal stripe-ordered state [40]. Ni sites with extra hole character (with respect to the d^9 magnetic rows) are in purple ($S = 0$), whereas Ni up and down spins in the magnetic rows are colored red and blue, respectively ($S = 1/2$). (c),(d) XAS data of $La_4Ni_3O_8$ measured in total fluorescence yield mode with polarization perpendicular and approximately parallel to the sample c-axis for (c) the Ni L-edge and (d) the O K-edge.

in Fig. 1(a), are ideal for testing the fundamental aspects of the analogy between layered nickelates and cuprates. This is because complications from rare-earth self-doping, c-axis coupling, and inhomogeneous samples are less severe in $R_4Ni_3O_8$ than in $RNiO_2$ [34,37,38].

In this Letter, we combine resonant inelastic x-ray scattering (RIXS) with first-principles calculations and theoretical modeling to characterize the magnetic exchange in trilayer $R_4Ni_3O_8$ that fall in the overdoped regime of cuprates in terms of electron count. We find a near-neighbor exchange of $J = 69(4)$ meV, in good accord with our first-principles calculations. This demonstrates that these reduced nickelates indeed have a strong super-exchange (within a factor of 2 of the cuprates). By comparing the O K-edge prepeak intensity to those of cuprates and infinite-layer nickelates, we argue that these trilayer materials are intermediate between cuprates and infinite-layer nickelates. Based on this, we suggest that electron-doping $R_4Ni_3O_8$ materials provides a compelling route to testing the relevance of superexchange for nickelate superconductivity.

$R_4Ni_3O_8$ (R = La, Pr) single crystals were prepared by synthesizing their parent Ruddlesden-Popper phases and reducing them in H_2/Ar gas as described previously [34,41]. The resulting samples are single-phase crystals with a tetragonal unit cell (I4/mmm space group) and lattice constants of $a = b = 3.97$ Å, $c = 26.1$ Å. The trilayer $R_4Ni_3O_8$ phase is shown in Fig. 1(a); Fig. 1(b) zooms in on the Ni-O planes. These samples have an effective hole doping of $\delta = 1/3$. Reciprocal space is indexed in terms of scattering vector $\boldsymbol{Q} = (2\pi/a, 2\pi/a, 2\pi/c)$. Both La and Pr materials are rather similar regarding their high- and medium-energy physics such as spin states and orbital polarization [34]. The primary difference is that $La_4Ni_3O_8$ (which exhibits strong antiferromagnetic spin fluctuations [47]) has stripe order that opens up a small insulating gap [34], whereas $Pr_4Ni_3O_8$ remains metallic without long-range order. Since the more ordered and insulating nature of $La_4Ni_3O_8$ compared to $Pr_4Ni_3O_8$ is expected to give sharper magnetic RIXS spectra, we focus on the former material for this paper.

We used XAS to confirm the expected electronic properties of the $La_4Ni_3O_8$ samples. The Ni L-edge spectrum from 846–878 eV is shown in Fig. 1(c). The strongest feature around 850 eV is the La M_4 edge, which is followed by the Ni L_3 and L_2 edges at 852 and 870 eV, respectively. Substantial linear dichroism is apparent, especially at the L_2 edge where the spectrum is not obscured by the La M_4 edge, indicating that the unoccupied $3d$ states are primarily $x^2 - y^2$ in character [34]. The overall spectral shape is very similar to that seen in cuprates [48–50], consistent with a $d^9 \underline{L}$ configuration, with no indication for a high-spin d^8 component of the holes [34]. This is reasonable, since the planar coordination of Ni leads to a large splitting between the $x^2 - y^2$ and $3z^2 - r^2$ states, which is expected to out-compete the Hunds exchange coupling, thus favoring a low-spin ground state [51]. The O K-edge spectrum around 525–545 eV in Fig. 1(d) shows a prepeak feature around 530 eV, which is known to indicate hybridization between the Ni $3d$ and O $2p$ states [34,48,49]. Our measurements find that this prepeak has a strong linear dichroism as well, as observed in cuprates [49].

We then performed RIXS to study the low-energy degrees of freedom. High-energy-resolution RIXS measurements were performed at I21 at the Diamond Light Source with a resolution of 45 meV and at NSLS-II with a resolution of 30 meV. All RIXS data shown were taken at a temperature of 20 K using a fixed horizontal scattering angle of $2\theta = 154°$ and x-ray polarization within the horizontal scattering plane (π polarization). Different momenta were accessed by rotating the sample about the vertical axis, such that the projection of the scattering vector varies. $(H, 0)$ and (H, H) scattering planes were accessed by rotating the sample about its azimuthal angle. Figure 2 plots low-energy RIXS spectra of $La_4Ni_3O_8$ as a function of $\boldsymbol{Q}$. A relatively strong elastic line is present for

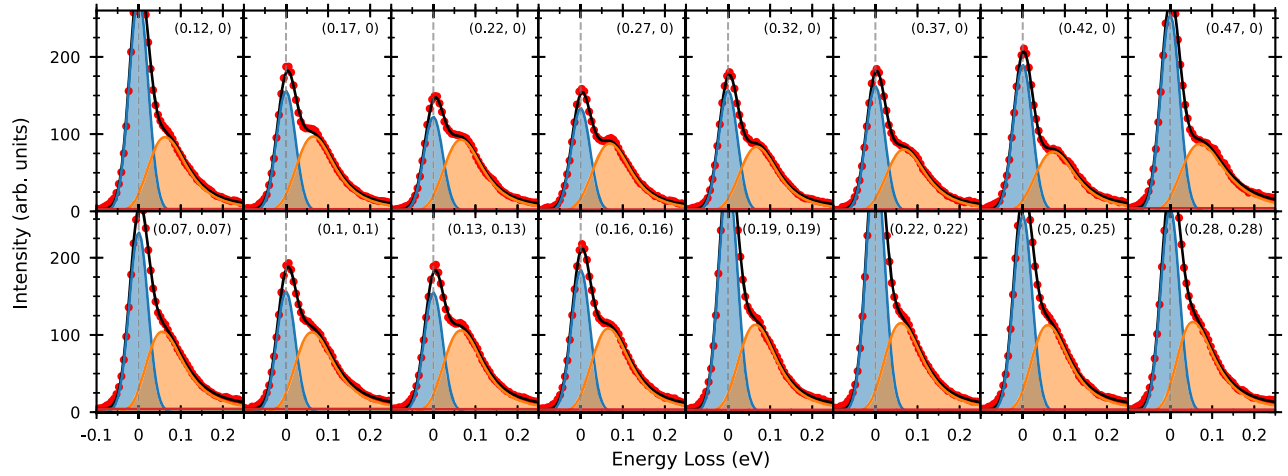FIG. 2. RIXS spectra of La$_4$Ni$_3$O$_8$ as a function of $\boldsymbol{Q}$ at the resonant energy of the magnon, 852.7 eV [41]. Data are shown as red points, and the fit is shown as a black line, which is composed of the magnetic excitation in orange and the elastic line in blue. The in-plane $\boldsymbol{Q}$ of the measured spectrum is denoted in the top right of each panel.

all $\boldsymbol{Q}$ likely arising from apical oxygen removal during sample preparation, which induces internal strain in the samples. In the 70–90 meV energy range, a weakly dispersive, damped feature is observed. Based on the energy of the feature, this could either be magnetic or the bond-stretching phonon common to complex oxides [52–56]. It is known, however, that the intensity of the bond-stretching phonon increases like $|\boldsymbol{Q}|^2$, inconsistent with what we find [55,56] (see Fig. 2). The peak also resonates slightly above the Ni L edge [41], which is also consistent with a magnetic origin [52]. On the basis of these observations, we assign this feature to magnetic excitations. Further supporting this assignment, we note that Pr$_4$Ni$_3$O$_8$ spectra exhibit a weaker, more damped paramagnon excitation, which is expected, as this compound is metallic with spin-glass behavior [41,57]. Below, we will demonstrate a consistency between this mode and analytical modeling and density functional theory (DFT).

In order to analyze the magnetic dispersion, we fit the low-energy RIXS spectra with the sum of a zero-energy Gaussian fixed to the experimental energy resolution in order to account for the elastic line and a damped harmonic oscillator to capture the magnetic excitation [41]. To model the magnetic interactions, we expect a leading contribution from the nearest-neighbor in-plane Ni-O-Ni super-exchange, J. We further know that La$_4$Ni$_3$O$_8$, like some other nickelates and cuprates, has a striped ground state with both spin and charge character, with an in-plane wave vector of $\boldsymbol{Q} = (1/3, 1/3)$ [40,58]. This diagonal stripe order is illustrated in Fig. 1(b) [41]. In each plane, we have two antiparallel spin rows (corresponding to d^9) separated by an antiphase domain wall (corresponding to nonmagnetic d^8). This gives rise to six spins in the magnetic unit cell in a given trilayer, which we label as spins 1–6. Nearest-neighbor spins within the planes in a given stripe are coupled by the superexchange J, which we

expect to be the strongest interaction. The antiphase domain wall is due to coupling between the magnetic stripes. There are two potential couplings (super-super-exchange), but we only expect one of them (the one along the tetragonal axes) to be significant, as the other involves a 90 degree pathway [59]. As the planes are antiferro-magnetically coupled [58], this gives rise to a positive J_z coupling between successive layers (there is no evidence for significant magnetic coupling between the trilayers [58], so our model deals with only a single trilayer). We solved the resulting Heisenberg model in the spin-wave approximation [60], which yields three dispersive modes (split by J_z), which we term the acoustic, middle, and optic modes [41]. The energy of each of these three modes changes with in-plane momentum, and the relative intensity of the modes is modulated by the out-of-plane momentum, which varies with in-plane momentum due to our fixed-scattering-angle configuration. From cuprates, we antici-pate that the interlayer coupling will be of order 10 meV, below our energy resolution [61,62]. On this basis, we analyzed our data in terms of the sum of the three magnon modes. The RIXS intensity for a particular acoustic, middle, or optic magnetic mode n in the π-σ polarization channel is given by [63]

$$I_n(\boldsymbol{Q}) = \left| \sum_i \boldsymbol{k}_{\text{in}} \cdot \boldsymbol{M}_{n,\boldsymbol{Q}}(\boldsymbol{r}_i) \right|^2, \qquad (1)$$

where $\boldsymbol{k}_{\text{in}}$ is the incident wave vector and $\boldsymbol{M}_{n,\boldsymbol{Q}}(\boldsymbol{r}_i)$ is the magnetization vector at site i (i.e., the eigenvector of the nth spin-wave mode at $\boldsymbol{Q}$). This vector is in-plane, since the ground-state moments are along c [58]. The final element of our model is to sum over the two tetragonal domains given the known magnetic twinning in La$_4$Ni$_3$O$_8$: $(H, K) \rightarrow (H, -K)$ [40,58]. We determined the energies and eigenvectors of these modes from the

resulting 12×12 secular matrix [41], and computed the weighted sum of the three modes at each Q [64]. To estimate the magnetic exchange parameters in $La_4Ni_3O_8$, we computed the energy of four different spin configurations in the above-mentioned magnetic cell [41], and then mapped these energies to a Heisenberg model. This was done using DFT in the generalized gradient approximation (GGA) implementation as provided in the WIEN2k code [65,66]. The experimentally determined insulating charge and spin stripe-ordered ground state [Fig. 1(b)] is obtained even at the GGA level, given that the exchange splitting is larger than the bandwidth in this state. Adding a U simply increases the size of the gap with respect to the GGA solution, but the nature of the ground state remains the same [37]. Results presented here are for GGA, but GGA + U results are presented in Ref. [41]. This yields $J = 71$ meV, $J_z = 13.6$ meV, and $J_1 = 10.6$ meV. We fix $J_z = 13.6$ meV in our model since, because of our resolution and contamination from the elastic line, we cannot accurately estimate it from experiment. We then vary J and J_1 to get the best fit. This fit yields $J = 69(4)$ meV and $J_1 = 17(4)$ meV in good agreement with theory, although the small difference in J (2 meV) is likely coincidental. These exchange values can be rationalized from the single-layer analytic relation (i.e., ignoring J_z) that $E_{mag} \sim 4S\sqrt{JJ_1}$, where E_{mag} is the zone-boundary magnon energy. We overplot the magnetic dispersion with our theory analysis in Fig. 3, showing a good level of agreement. The model also captures the observed softening that occurs as Q approaches $(-\frac{1}{3}, -\frac{1}{3})$. We also measured $Pr_4Ni_3O_8$ [41], which is similar to $La_4Ni_3O_8$, but metallic rather than insulating; the results show a lower-intensity damped magnetic excitation, which is expected in view of its metallicity [34] and the spin-glass behavior reported for
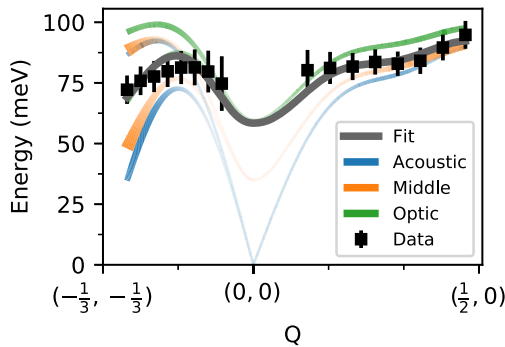
this material [57]. The paramagnon energy in $Pr_4Ni_3O_8$ is only slightly reduced compared to $La_4Ni_3O_8$. Again, this is similar to cuprates, where magnon-like excitations are seen for paramagnetic dopings [67].

Our rather large value of $J = 69(4)$ meV is the principal result of this Letter. This magnetic exchange is 2.5 times larger than that of the $1/3$ doped nickelate $La_{2-x}Sr_xNiO_4$, which also has a diagonal stripe state (with $S = 1$ d^8 magnetic rows and $S = 1/2$ d^7 domain walls), though the two have comparable J_1 [52,68,69]. J for $La_4Ni_3O_8$ is, in fact, within a factor of 2 of cuprates, which have among the largest superexchange of any known material [67,70–72]. This suggests, along with our XAS results, that these nickelates are strongly correlated charge-transfer materials. Two questions are apparent: Why is the superexchange in $La_4Ni_3O_8$ so large? And what is the relationship between trilayer nickelates and their infinite-layer counterparts?

Given the 180 degree Ni-O-Ni bonds in the d^9 nickelates, superexchange is the most likely mechanism for generating their exchange interactions, as in the cuprates. In the charge-transfer limit, the strength of this interaction scales as t_{pd}^4/Δ^3, where t_{pd} is the hopping between the transition metal $x^2 - y^2$ and oxygen $p\sigma$ orbitals, and $\Delta \equiv E_d - E_p$ is the energy difference between them. Large $p - d$ hopping and a small Δ implies a large ligand-hole character for the doped holes, as this is controlled by the ratio t_{pd}/Δ. We therefore fit the O K prepeak intensity to compare to the literature for $La_{2-x}Sr_xCuO_4$ [48] and $Nd_{1-x}Sr_xNiO_2$ [8] and show the results in Fig. 4. The prepeak in $Nd_{1-x}Sr_xNiO_2$ is significantly less prominent than in $La_4Ni_3O_8$ and $La_{2-x}Sr_xCuO_4$, but this appears to be primarily due to a broadened prepeak rather than a lower integrated spectral weight, the broadening perhaps due to a spatially varying doping. The relative integrated weight per doped hole is $1.00(2):1.74$ $(5):1.05(10)$ for $La_4Ni_3O_8:La_{2-x}Sr_xCuO_4:Nd_{1-x}Sr_xNiO_2$, and the equivalent ratios for the maximum prepeak

FIG. 3. Magnetic dispersion of $La_4Ni_3O_8$. Black points are the extracted energies of the magnetic excitation. The gray line is the fit to the experimental dispersion, which is composed of the weighted sum of three dispersive magnons, called the acoustic, middle, and optic modes, which are plotted as blue, orange, and green lines, respectively. The thicknesses of all three lines represent the predicted intensity of the modes [41]. The doubling of the modes from $(-\frac{1}{3}, -\frac{1}{3})$ to $(0,0)$ arises from magnetic twinning [41].
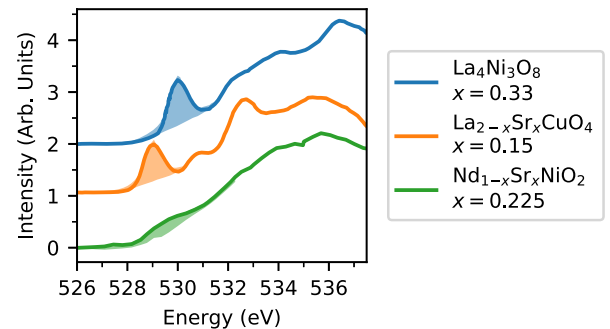

FIG. 4. Comparison of the O K-edge in-plane polarized prepeak intensity, indicative of oxygen-hybridized holes, between different $d^{9-\delta}$ materials. Solid lines are XAS or EELS. The data and background (line shape excluding the prepeak) for $Nd_{1-x}Sr_xNiO_2$ are from Ref. [8], and the data for $La_{2-x}Sr_xCuO_4$ are from Ref. [49]. Further details are provided in Ref. [41].

intensities are 1.00(4):1.85(9):0.37(6). The quoted errors are the uncertainties from the least-squares fitting algorithm. The largest systematic error likely arises from the doping inhomogeneity in the data from Ref. [8]. Thus, $La_4Ni_3O_8$ has somewhat less admixture than $La_{2-x}Sr_xCuO_4$, but the difference is not enough to expect qualitatively different physics. The ratio we determine is in good accord with our observed magnetic exchange in $La_4Ni_3O_8$ being around half that of the cuprates [67, 71–73]. This difference likely comes from Δ being larger in $La_4Ni_3O_8$ compared to $La_{2-x}Sr_xCuO_4$ (t_{pd} is comparable in the three materials) [74,75]. The situation in $NdNiO_2$ is less certain, given the large difference of the ratios (i.e., whether one considers the maximum intensity or the integrated weight). This will likely only be solved when higher-quality, more homogeneous $Nd_{1-x}Sr_xNiO_2$ samples are prepared and studied in detail. Still, it seems likely that the superexchange in $NdNiO_2$ is smaller, but still large enough that its potential contribution to superconductivity deserves serious consideration. Recent Raman scattering measurements estimate $J \approx 25$ meV [76], which is consistent with this and which likely arises from Δ being larger, though the enhanced c-axis coupling and the screening from the R $5d$ states, which are predicted to be partially occupied in $NdNiO_2$, could be playing a role as well.

In conclusion, we report the presence of a large superexchange $J = 69(4)$ meV in $La_4Ni_3O_8$—the first direct measurement of superexchange in a $d^{9-\delta}$ nickelate. This superexchange value is within a factor of 2 of values found in the cuprates, and this, coupled with a substantial O K prepeak, establishes the charge-transfer nature of this $d^{9-\delta}$ nickelate with substantial $d - p$ mixing. By comparing the O K-edge XAS spectra of $La_4Ni_3O_8$ to that of the cuprates and the infinite-layer nickelate, we establish that trilayer nickelates represent a case that is intermediate between them. This result is interesting in view of the widespread belief that increasing magnetic superexchange might promote higher-T_c superconductivity [4,34,77]. Studying a series of layered nickelates would also provide a route to testing the relevance of superexchange to nickelate superconductivity given the variation in their nominal Ni valence.

---

[*]CAS Key Laboratory of Magnetic Materials and Devices, Ningbo Institute of Materials Technology and Engineering, Chinese Academy of Sciences, Ningbo 315201, China, and Zhejiang Province Key Laboratory of Magnetic Materials and Application Technology, Ningbo Institute of Materials Technology and Engineering, Chinese Academy of Sciences, Ningbo 315201, China.
[†]liuxr@shanghaitech.edu.cn
[‡]norman@anl.gov
[§]mdean@bnl.gov

[1] J. G. Bednorz and K. A. Müller, Possible high T_c superconductivity in the Ba-La-Cu-O system, Z. Phys. B **64**, 189 (1986).

[2] M. R. Norman, Materials design for new superconductors, Rep. Prog. Phys. **79**, 074502 (2016).

[3] R. Adler, C.-J. Kang, C.-H. Yee, and G. Kotliar, Correlated materials design: Prospects and challenges, Rep. Prog. Phys. **82**, 012504 (2019).

[4] M. R. Norman, Entering the nickel age of superconductivity, Physics **13**, 85 (2020).

[5] V. I. Anisimov, D. Bukhvalov, and T. M. Rice, Electronic structure of possible nickelate analogs to the cuprates, Phys. Rev. B **59**, 7901 (1999).

[6] K.-W. Lee and W. E. Pickett, Infinite-layer $LaNiO_2$: Ni^{1+} is not Cu^{2+}, Phys. Rev. B **70**, 165109 (2004).

[7] D. Li, K. Lee, B. Y. Wang, M. Osada, S. Crossley, H. R. Lee, Y. Cui, Y. Hikita, and H. Y. Hwang, Superconductivity in an infinite-layer nickelate, Nature (London) **572**, 624 (2019).

[8] B. H. Goodge, D. Li, K. Lee, M. Osada, B. Y. Wang, G. A. Sawatzky, H. Y. Hwang, and L. F. Kourkoutis, Doping evolution of the Mott–Hubbard landscape in infinite-layer nickelates, Proc. Natl. Acad. Sci. U.S.A. **118**, e2007683118 (2021).

[9] M. Osada, B. Y. Wang, B. H. Goodge, K. Lee, H. Yoon, K. Sakuma, D. Li, M. Miura, L. F. Kourkoutis, and H. Y. Hwang, A superconducting praseodymium nickelate with infinite layer structure, Nano Lett. **20**, 5735 (2020).

[10] S. Zeng, C. S. Tang, X. Yin, C. Li, M. Li, Z. Huang, J. Hu, W. Liu, G. J. Omar, H. Jani, Z. S. Lim, K. Han, D. Wan, P.

Yang, S. J. Pennycook, A. T. S. Wee, and A. Ariando, Phase Diagram and Superconducting Dome of Infinite-Layer $Nd_{1-x}Sr_xNiO_2$ Thin Films, Phys. Rev. Lett. **125**, 147003 (2020).

[11] M. Hepting, D. Li, C. Jia, H. Lu, E. Paris, Y. Tseng, X. Feng, M. Osada, E. Been, Y. Hikita *et al.*, Electronic structure of the parent compound of superconducting infinite-layer nickelates, Nat. Mater. **19**, 381 (2020).

[12] B.-X. Wang, H. Zheng, E. Krivyakina, O. Chmaissem, P. P. Lopes, J. W. Lynn, L. C. Gallington, Y. Ren, S. Rosenkranz, J. Mitchell *et al.*, Synthesis and characterization of bulk $Nd_{1-x}Sr_xNiO_2$ and $Nd_{1-x}Sr_xNiO_3$, Phys. Rev. Mater. **4**, 084409 (2020).

[13] A. S. Botana and M. R. Norman, Similarities and differences between $LaNiO_2$ and $CaCuO_2$ and Implications for Superconductivity, Phys. Rev. X **10**, 011024 (2020).

[14] H. Sakakibara, H. Usui, K. Suzuki, T. Kotani, H. Aoki, and K. Kuroki, Model Construction and a Possibility of Cupratelike Pairing in a New d^9 Nickelate Superconductor (Nd, Sr)NiO_2, Phys. Rev. Lett. **125**, 077003 (2020).

[15] M. Jiang, M. Berciu, and G. A. Sawatzky, Critical Nature of the Ni Spin State in Doped $NdNiO_2$, Phys. Rev. Lett. **124**, 207004 (2020).

[16] Y. Nomura, M. Hirayama, T. Tadano, Y. Yoshimoto, K. Nakamura, and R. Arita, Formation of a two-dimensional single-component correlated electron system and band engineering in the nickelate superconductor $NdNiO_2$, Phys. Rev. B **100**, 205138 (2019).

[17] X. Wu, D. Di Sante, T. Schwemmer, W. Hanke, H. Y. Hwang, S. Raghu, and R. Thomale, Robust $d_{x^2-y^2}$-wave superconductivity of infinite-layer nickelates, Phys. Rev. B **101**, 060504(R) (2020).

[18] H. Zhang, L. Jin, S. Wang, B. Xi, X. Shi, F. Ye, and J.-W. Mei, Effective hamiltonian for nickelate oxides $Nd_{1-x}Sr_xNiO_2$, Phys. Rev. Research **2**, 013214 (2020).

[19] G.-M. Zhang, Y.-f. Yang, and F.-C. Zhang, Self-doped Mott insulator for parent compounds of nickelate superconductors, Phys. Rev. B **101**, 020501(R) (2020).

[20] P. Werner and S. Hoshino, Nickelate superconductors: Multiorbital nature and spin freezing, Phys. Rev. B **101**, 041104(R) (2020).

[21] L.-H. Hu and C. Wu, Two-band model for magnetism and superconductivity in nickelates, Phys. Rev. Research **1**, 032046(R) (2019).

[22] Y.-H. Zhang and A. Vishwanath, Type-II $t-J$ model in superconducting nickelate $Nd_{1-x}Sr_xNiO_2$, Phys. Rev. Research **2**, 023112 (2020).

[23] Z. Liu, Z. Ren, W. Zhu, Z. Wang, and J. Yang, Electronic and magnetic structure of infinite-layer $NdNiO_2$: Trace of antiferromagnetic metal, npj Quantum Mater. **5**, 1 (2020).

[24] J. Karp, A. S. Botana, M. R. Norman, H. Park, M. Zingl, and A. Millis, Many-Body Electronic Structure of $NdNiO_2$ and $CaCuO_2$, Phys. Rev. X **10**, 021061 (2020).

[25] E. Been, W.-S. Lee, H. Y. Hwang, Y. Cui, J. Zaanen, T. Devereaux, B. Moritz, and C. Jia, Theory of Rare-Earth Infinite Layer Nickelates, arXiv:2002.12300 [Phys. Rev. X (to be published)].

[26] Z.-J. Lang, R. Jiang, and W. Ku, Where do the doped hole carriers reside in the new superconducting nickelates? arXiv:2005.00022.

[27] Y. Wang, C.-J. Kang, H. Miao, and G. Kotliar, Hund's metal physics: From $SrNiO_2$ to $LaNiO_2$, Phys. Rev. B **102**, 161118(R) (2020).

[28] Y. Nomura, T. Nomoto, M. Hirayama, and R. Arita, Magnetic exchange coupling in cuprate-analog d^9 nickelates, Phys. Rev. Research **2**, 043144 (2020).

[29] J. Kapeghian and A. S. Botana, Electronic structure and magnetism in infinite-layer nickelates $RNiO_2$ ($R = La - Lu$), Phys. Rev. B **102**, 205130 (2020).

[30] G. A. Sawatzky, Superconductivity seen in a non-magnetic nickel oxide, Nature (London) **572**, 592 (2019).

[31] M. Crespin, P. Levitz, and L. Gatineau, Reduced forms of $LaNiO_3$ perovskite. Part 1. Evidence for new phases: $La_2Ni_2O_5$ and $LaNiO_2$, J. Chem. Soc., Faraday Trans. 2 **79**, 1181 (1983).

[32] M. A. Hayward, M. A. Green, M. J. Rosseinsky, and J. Sloan, Sodium hydride as a powerful reducing agent for topotactic oxide deintercalation: Synthesis and characterization of the nickel(I) oxide $LaNiO_2$, J. Am. Chem. Soc. **121**, 8843 (1999).

[33] M. A. Hayward and M. J. Rosseinsky, Synthesis of the infinite layer Ni(I) phase $NdNiO_{2+x}$ by low temperature reduction of $NdNiO_3$ with sodium hydride, Solid State Sci. **5**, 839 (2003).

[34] J. Zhang, A. Botana, J. Freeland, D. Phelan, H. Zheng, V. Pardo, M. Norman, and J. Mitchell, Large orbital polarization in a metallic square-planar nickelate, Nat. Phys. **13**, 864 (2017).

[35] P. W. Anderson, The resonating valence bond state in La_2CuO_4 and superconductivity, Science **235**, 1196 (1987).

[36] D. J. Scalapino, A common thread: The pairing interaction for unconventional superconductors, Rev. Mod. Phys. **84**, 1383 (2012).

[37] V. V. Poltavets, K. A. Lokshin, A. H. Nevidomskyy, M. Croft, T. A. Tyson, J. Hadermann, G. Van Tendeloo, T. Egami, G. Kotliar, N. ApRoberts-Warren, A. P. Dioguardi, N. J. Curro, and M. Greenblatt, Bulk Magnetic Order in a Two-Dimensional Ni^{1+}/Ni^{2+} (d^9/d^8) Nickelate, Isoelectronic with Superconducting Cuprates, Phys. Rev. Lett. **104**, 206403 (2010).

[38] A. S. Botana, V. Pardo, W. E. Pickett, and M. R. Norman, Charge ordering in Ni^{1+}/Ni^{2+} nickelates: $La_4Ni_3O_8$ and $La_3Ni_2O_6$, Phys. Rev. B **94**, 081105(R) (2016).

[39] K. Momma and F. Izumi, VESTA3 for three-dimensional visualization of crystal, volumetric and morphology data, J. Appl. Crystallogr. **44**, 1272 (2011).

[40] J. Zhang, Y.-S. Chen, D. Phelan, H. Zheng, M. R. Norman, and J. F. Mitchell, Stacked charge stripes in the quasi-2D trilayer nickelate $La_4Ni_3O_8$, Proc. Natl. Acad. Sci. U.S.A. **113**, 8945 (2016).

[41] See Supplemental Material at http://link.aps.org/supplemental/10.1103/PhysRevLett.126.087001 for details of RIXS data on $Pr_4Ni_3O_8$, our theoretical model for spin excitations, details on our first-principles calculations of magnetic exchange, additional information about sample synthesis and a description of the least-squares data fitting, which also includes Refs. [42–46].

[42] J. P. Perdew, K. Burke, and M. Ernzerhof, Generalized Gradient Approximation made Simple, Phys. Rev. Lett. **77**, 3865 (1996).

[43] E. R. Ylvisaker, W. E. Pickett, and K. Koepernik, Anisotropy and magnetism in the LSDA + U method, Phys. Rev. B **79**, 035103 (2009).

[44] P. Virtanen *et al.* and SciPy 1.0 Contributors, SciPy 1.0: Fundamental algorithms for scientific computing in Python, Nat. Methods **17**, 261 (2020).

[45] H. Chen and A. J. Millis, Spin-density functional theories and their $+U$ and $+J$ extensions: A comparative study of transition metals and transition metal oxides, Phys. Rev. B **93**, 045133 (2016).

[46] S. Ryee and M. J. Han, The effect of double counting, spin density, and hund interaction in the different DFT $+ U$ functionals, Sci. Rep. **8**, 1 (2018).

[47] N. ApRoberts-Warren, A. P. Dioguardi, V. V. Poltavets, M. Greenblatt, P. Klavins, and N. J. Curro, Critical spin dynamics in the antiferromagnet $La_4Ni_3O_8$ from ^{139}La nuclear magnetic resonance, Phys. Rev. B **83**, 014402 (2011).

[48] C. T. Chen, F. Sette, Y. Ma, M. S. Hybertsen, E. B. Stechel, W. M. C. Foulkes, M. Schulter, S.-W. Cheong, A. S. Cooper, L. W. Rupp, B. Batlogg, Y. L. Soo, Z. H. Ming, A. Krol, and Y. H. Kao, Electronic States in $La_{2-x}Sr_xCuO_{4+\delta}$ Probed by Soft-X-Ray Absorption, Phys. Rev. Lett. **66**, 104 (1991).

[49] C. T. Chen, L. H. Tjeng, J. Kwo, H. L. Kao, P. Rudolf, F. Sette, and R. M. Fleming, Out-of-Plane Orbital Characters of Intrinsic and Doped Holes in $La_{2-x}Sr_xCuO_4$, Phys. Rev. Lett. **68**, 2543 (1992).

[50] N. B. Brookes, G. Ghiringhelli, A.-M. Charvet, A. Fujimori, T. Kakeshita, H. Eisaki, S. Uchida, and T. Mizokawa, Stability of the Zhang-Rice Singlet with Doping in Lanthanum Strontium Copper Oxide across the Superconducting Dome and above, Phys. Rev. Lett. **115**, 027002 (2015).

[51] G. Fabbris, D. Meyers, J. Okamoto, J. Pelliciari, A. S. Disa, Y. Huang, Z.-Y. Chen, W. B. Wu, C. T. Chen, S. Ismail-Beigi, C. H. Ahn, F. J. Walker, D. J. Huang, T. Schmitt, and M. P. M. Dean, Orbital Engineering in Nickelate Heterostructures Driven by Anisotropic Oxygen Hybridization rather than Orbital Energy Levels, Phys. Rev. Lett. **117**, 147401 (2016).

[52] G. Fabbris, D. Meyers, L. Xu, V. M. Katukuri, L. Hozoi, X. Liu, Z.-Y. Chen, J. Okamoto, T. Schmitt, A. Uldry, B. Delley, G. D. Gu, D. Prabhakaran, A. T. Boothroyd, J. van den Brink, D. J. Huang, and M. P. M. Dean, Doping Dependence of Collective Spin and Orbital Excitations in the Spin-1 Quantum Antiferromagnet $La_{2-x}Sr_xNiO_4$ observed by X Rays, Phys. Rev. Lett. **118**, 156402 (2017).

[53] D. Betto, Y. Y. Peng, S. B. Porter, G. Berti, A. Calloni, G. Ghiringhelli, and N. B. Brookes, Three-dimensional dispersion of spin waves measured in NiO by resonant inelastic x-ray scattering, Phys. Rev. B **96**, 020409(R) (2017).

[54] A. Nag, H. C. Robarts, F. Wenzel, J. Li, H. Elnaggar, R.-P. Wang, A. C. Walters, M. García-Fernández, F. M. F. de Groot, M. W. Haverkort, and K.-J. Zhou, Many-Body Physics of Single and Double Spin-Flip Excitations in NiO, Phys. Rev. Lett. **124**, 067202 (2020).

[55] J. Q. Lin, H. Miao, D. G. Mazzone, G. D. Gu, A. Nag, A. C. Walters, M. García-Fernández, A. Barbour, J. Pelliciari, I. Jarrige, M. Oda, K. Kurosawa, N. Momono, K.-J. Zhou, V. Bisogni, X. Liu, and M. P. M. Dean, Strongly Correlated Charge Density Wave in $La_{2-x}Sr_xCuO_4$ Evidenced by Doping-Dependent Phonon Anomaly, Phys. Rev. Lett. **124**, 207005 (2020).

[56] T. P. Devereaux, A. M. Shvaika, K. Wu, K. Wohlfeld, C. J. Jia, Y. Wang, B. Moritz, L. Chaix, W.-S. Lee, Z.-X. Shen, G. Ghiringhelli, and L. Braicovich, Directly Characterizing the Relative Strength and Momentum Dependence of Electron-Phonon Coupling Using Resonant Inelastic X-Ray Scattering, Phys. Rev. X **6**, 041019 (2016).

[57] S. Huangfu, Z. Guguchia, D. Cheptiakov, X. Zhang, H. Luetkens, D. J. Gawryluk, T. Shang, F. O. von Rohr, and A. Schilling, Short-range magnetic interactions and spin-glass behavior in the quasi-two-dimensional nickelate $Pr_4Ni_3O_8$, Phys. Rev. B **102**, 054423 (2020).

[58] J. Zhang, D. M. Pajerowski, A. S. Botana, H. Zheng, L. Harriger, J. Rodriguez-Rivera, J. P. C. Ruff, N. J. Schreiber, B. Wang, Y.-S. Chen, W. C. Chen, M. R. Norman, S. Rosenkranz, J. F. Mitchell, and D. Phelan, Spin Stripe Order in a Square Planar Trilayer Nickelate, Phys. Rev. Lett. **122**, 247201 (2019).

[59] Diagrams for the exchange pathways are shown in Ref. [41].

[60] E. W. Carlson, D. X. Yao, and D. K. Campbell, Spin waves in striped phases, Phys. Rev. B **70**, 064505 (2004).

[61] D. Reznik, P. Bourges, H. F. Fong, L. P. Regnault, J. Bossy, C. Vettier, D. L. Milius, I. A. Aksay, and B. Keimer, Direct observation of optical magnons in $YBa_2Cu_3O_{6.2}$, Phys. Rev. B **53**, R14741 (1996).

[62] M. P. M. Dean, A. J. A. James, A. C. Walters, V. Bisogni, I. Jarrige, M. Hücker, E. Giannini, M. Fujita, J. Pelliciari, Y. B. Huang, R. M. Konik, T. Schmitt, and J. P. Hill, Itinerant effects and enhanced magnetic interactions in Bi-based multilayer cuprates, Phys. Rev. B **90**, 220506(R) (2014).

[63] M. W. Haverkort, Theory of Resonant Inelastic X-Ray Scattering by Collective Magnetic Excitations, Phys. Rev. Lett. **105**, 167404 (2010).

[64] Our spin-wave approach does not include any quantum renormalization factor, Z_c, of the spin-wave energy, and this difference should be accounted for when comparing to cuprates when Z_c has been accounted for, which requires exchange values $Z_c \sim 1.18$ times larger to reproduce the same magnon energy [72,78].

[65] P. Blaha, K. Schwarz, G. K. H. Madsen, D. Kvasnicka, J. Luitz, R. Laskowski, F. Tran, and L. D. Marks, WIEN2k, *An Augmented Plane Wave+Local Orbitals Program for Calculating Crystal Properties* (Karlheinz Schwarz, Techn. Universität Wien, Austria, 2018).

[66] P. Blaha, K. Schwarz, F. Tran, R. Laskowski, G. K. H. Madsen, and L. D. Marks, WIEN2k: An APW + lo program for calculating the properties of solids, J. Chem. Phys. **152**, 074101 (2020).

[67] M. P. M. Dean, G. Dellea, R. Springell, F. Yakhou-Harris, K. Kummer, N. Brookes, X. Liu, Y. Sun, J. Strle, T. Schmitt *et al.*, Persistence of magnetic excitations in $La_{2-x}Sr_xCuO_4$ from the undoped insulator to the heavily overdoped non-superconducting metal, Nat. Mater. **12**, 1019 (2013).

[68] A. T. Boothroyd, D. Prabhakaran, P. G. Freeman, S. J. S. Lister, M. Enderle, A. Hiess, and J. Kulda, Spin dynamics in stripe-ordered $La_{5/3}Sr_{1/3}NiO_4$, Phys. Rev. B **67**, 100407(R) (2003).

[69] H. Woo, A. T. Boothroyd, K. Nakajima, T. G. Perring, C. D. Frost, P. G. Freeman, D. Prabhakaran, K. Yamada, and J. M. Tranquada, Mapping spin-wave dispersions in stripe-ordered La$_{2-x}$Sr$_x$NiO$_4$ ($x = 0.275, 0.333$), Phys. Rev. B **72,** 064437 (2005).

[70] R. Coldea, S. M. Hayden, G. Aeppli, T. G. Perring, C. D. Frost, T. E. Mason, S.-W. Cheong, and Z. Fisk, Spin Waves and Electronic Interactions in La$_2$CuO$_4$, Phys. Rev. Lett. **86,** 5377 (2001).

[71] M. Le Tacon, G. Ghiringhelli, J. Chaloupka, M. M. Sala, V. Hinkov, M. Haverkort, M. Minola, M. Bakr, K. Zhou, S. Blanco-Canosa *et al.*, Intense paramagnon excitations in a large family of high-temperature superconductors, Nat. Phys. **7,** 725 (2011).

[72] Y. Peng, G. Dellea, M. Minola, M. Conni, A. Amorese, D. Di Castro, G. De Luca, K. Kummer, M. Salluzzo, X. Sun *et al.*, Influence of apical oxygen on the extent of in-plane exchange interaction in cuprate superconductors, Nat. Phys. **13,** 1201 (2017).

[73] M. Dean, R. Springell, C. Monney, K. Zhou, J. Pereiro, I. Božović, B. Dalla Piazza, H. Rønnow, E. Morenzoni, J. Van Den Brink *et al.*, Spin excitations in a single La$_2$CuO$_4$ layer, Nat. Mater. **11,** 850 (2012).

[74] E. M. Nica, J. Krishna, R. Yu, Q. Si, A. S. Botana, and O. Erten, Theoretical investigation of superconductivity in trilayer square-planar nickelates, Phys. Rev. B **102,** 020504 (R) (2020).

[75] A. K. McMahan, J. F. Annett, and R. M. Martin, Cuprate parameters from numerical wannier functions, Phys. Rev. B **42,** 6268 (1990).

[76] Y. Fu, L. Wang, H. Cheng, S. Pei, X. Zhou, J. Chen, S. Wang, R. Zhao, W. Jiang, C. Liu *et al.*, Core-level x-ray photoemission and Raman spectroscopy studies on electronic structures in Mott-Hubbard type nickelate oxide NdNiO$_2$, arXiv:1911.03177.

[77] A. S. Botana, V. Pardo, and M. R. Norman, Electron doped layered nickelates: Spanning the phase diagram of the cuprates, Phys. Rev. Mater. **1,** 021801(R) (2017).

[78] R. R. P. Singh, Thermodynamic parameters of the $t = 0$, spin-1/2 square-lattice Heisenberg antiferromagnet, Phys. Rev. B **39,** 9760 (1989).